Trees
DOI 10.1007/s00468-014-1076-0

ORIGINAL PAPER

Determining parameters related to the likelihood of failure of red oak (*Quercus rubra* L.) from winching tests

Brian Kane

Received: 8 July 2014 / Revised: 9 August 2014 / Accepted: 14 August 2014

Abstract
Key message **This study provides data necessary to develop mechanistic models of the failure of open-grown trees. The literature contains few such data. Some results contrast previous studies on conifers.**
Abstract In cities and towns, tree failure can cause damage and injury. Few studies have considered large, open-grown trees when measuring parameters related to tree failure. To measure elastic modulus and maximum bending moment and stress, we winched red oaks (*Quercus rubra* L.), including some with co-dominant stems and others with extant decay. To simulate decay in a subsample of trees, we cut voids in the trunk before pulling trees to failure. Maximum bending moment was greatest for uprooted trees, but maximum bending and shear stresses were greatest for trees that failed in the crown in the vicinity of branches. The likelihood of failure at a void or area of extant decay increased as the loss in area moment of inertia increased. The moduli of elasticity and rupture of specimens taken from trees were greater than values measured on the trees themselves. Failure at the union of co-dominant stems only occurred when we pulled them apart, loading them perpendicular to the plane bifurcating the union. Some of the results are inconsistent with previous work on conifers; more data on open-grown trees are necessary to develop mechanistic models to predict tree failure.

Keywords Co-dominant stem · Decay · Decurrent · Tree failure · Tree pulling

Introduction

In cities and towns, trees provide many benefits (Nowak and Dwyer 2000), which accrue mostly from larger trees (Nowak et al. 2002). However, if they fail, large trees are more likely to cause property damage and personal injury. From 1995 to 2007, 407 people died as a result of wind-related tree failures in the United States (Schmidlin 2009) and concomitant litigation (Mortimer and Kane 2004) can be costly. Assessing the likelihood of tree failure presents many challenges. Foresters have developed mechanistic models for forest- or plantation-grown conifers of excurrent form that have proved somewhat reliable (Gardiner et al. 2008). Empirical parameters support such models and have been collected for many years, often by pulling trees to failure (Peltola 2006; Nicoll et al. 2006). Mechanistic models to estimate the likelihood of failure of open-grown trees (Brudi and van Wassanaer 2001) have not been rigorously validated. Developing a mechanistic model to predict failure of open-grown trees will help reduce the likelihood of personal injury and property damage.

Few tree pulling studies have considered large, open-grown deciduous trees (Kane and Clouston 2008; Kane et al. 2014), which typically develop a decurrent form. Such trees are common in towns and cities, planted along streets or in residential yards. Some studies have shown that predictive relationships developed for forest- or plantation-grown conifers of excurrent form do not apply to open-grown trees of decurrent form (Kane and James 2011; Kane et al. 2014). For example, large branches typical of many open-grown trees can influence their sway response

Communicated by T. Fourcaud.

B. Kane (✉)
Department of Environmental Conservation, University of Massachusetts, 160 Holdsworth Way, Amherst, MA 01003, USA
e-mail: bkane@eco.umass.edu

Published online: 10 September 2014

(Ciftci et al. 2013) and, if they become co-dominant with the trunk and develop bark inclusions, weaken the union (Kane and Clouston 2008).

Many parameters are needed to develop a mechanistic model of failure of an open-grown tree, but most have not been well quantified by rigorous experimentation. This may be due in part to logistic challenges of destructively testing large trees growing in residential neighborhoods. Many open-grown trees also develop structural defects like decay and poor branch unions that predispose trees to failure. Tree pulling studies of forest- or plantation-grown trees usually exclude trees with apparent defects (Fredericksen et al. 1993; Achim et al. 2005; Peterson and Claassen 2013). Quantifying the effect of such defects is another critical aspect of predicting failure, but few studies have undertaken the work on full-size trees (Kane and Clouston 2008).

Two common defects on open-grown trees in residential neighborhoods are decay and weak branch unions. Conventional methods of assessing the likelihood of failure from decay can be inaccurate (Kane and Ryan 2004; Ruel et al. 2010). Recent approaches (Ciftci et al. 2014) have attempted to address this, yet no studies have destructively sampled large open-grown trees to empirically assess the effect of decay. More studies have investigated the strength of branch unions, which decreases (1) as the ratio of branch to trunk diameter increases (Gilman 2003; Kane et al. 2008) and (2) when included bark is present (Smiley 2003). Fewer studies have tested larger branches and trees (Lilly and Sydnor 1995; Kane and Clouston 2008). Recent insights have cautioned that not all branch unions constitute a defect (Slater and Ennos 2013). Investigations of branch unions, however, have universally applied loads perpendicular to the plane that bifurcates the union, inducing tensile stress perpendicular to the plane. Since wind can load branch unions from many directions, it is important to test whether the direction of loading affects the strength of the union.

Our objectives were to (1) investigate patterns of failure in trees with decurrent form, (2) determine their elastic modulus and maximum bending moment and stress, and (3) ascertain the effect of structural defects (co-dominant stems and decay) on yield stress and the likelihood of failure.

Methods

Field tests

We used a pulling test similar to that described in (Peltola 2006) on 55 red oaks (*Quercus rubra* L.) growing in a forested stand along an abandoned road in Pelham, MA,

Table 1 Means and standard deviations of (a) tree morphometric data and (b) test parameters for 55 red oaks

Parameter	Units	Mean	Std dev
(a)			
DBH	m	0.37	0.07
Tree height	m	19.3	2.65
Crown width	m	10.0	2.41
Crown height	m	10.6	2.83
Crown height/tree height	–	0.54	0.09
Tree height/DBH	–	53.5	8.80
(b)			
Angle of pull (θ)	°	76.1	4.18
Trunk diameter at load height	m	0.18	0.03
Load height	m	12.2	2.22
Load height/tree height	–	0.63	0.07
Load height–height of crown base	m	3.55	2.18
I_{LOSS}^{a} of sawn voids[b]		43 %	22 %
I_{LOSS} of trees with extant decay[c]		41 %	23 %

[a] Loss in area moment of inertia (Eq. 2 in the text)

[b] $n = 28$

[c] $n = 5$

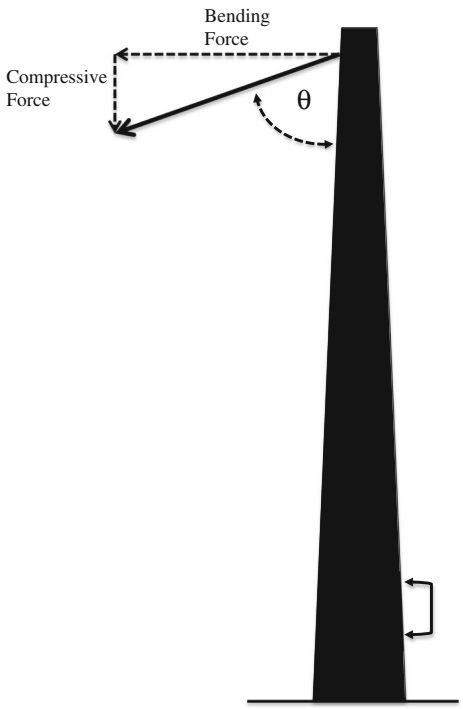

Fig. 1 Schematic diagram (not to scale) illustrating the angle of attachment (θ) of the applied load (*solid arrow*) resolved into components (*dashed arrows*) perpendicular (Bending Force) and parallel (Compressive Force) to the trunk, and the strain meter (*bracket with arrowheads*) attached to the trunk. The height of the mid-point of the strain meter was approximately one meter above ground. The load cell was anchored to the skidder that applied the load (not shown)

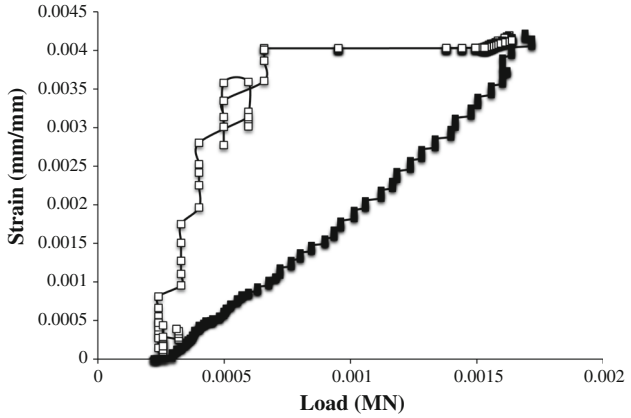

Fig. 2 An example of strains plotted against load while loading (*filled square*) and unloading (*unfilled square*) tree 42

USA (USDA Hardiness Zone 5A). The main difference was the rate of loading (which we describe in the following paragraph). Most trees had assumed a decurrent form following a heavy thinning of the stand 30 years prior (Table 1). Table 1 also includes parameters that describe the pulling test. To limit the bending moment induced by the offset mass of the crown during testing, we pruned branches back to stubs prior to testing. We attached a snatch block (McKissick Light Champion model 419) to the tree with an Ultrex sling (1.9 cm diameter, Yale Cordage) at greater than half the height of the tree, above the crown base. We pulled trees using a skidder (John Deere model 440D) with a hydraulic winch and 61 m of Vectrus winch line (1.3 cm diameter, Yale Cordage). The rope passed through the snatch block and was attached to a load cell (Dillon EDXtreme, Weigh-Tronix, Fairmont, MN, USA) that recorded loads (accurate to 44 N) at 10 Hz. To calculate bending moment and axial force, we doubled the recorded loads since the rope pass through the block; doing so overestimated the actual load because of friction in the block. We assumed that the effect of friction was negligible. We measured the angle between the applied load and the trunk (θ) and resolved loads into components parallel and perpendicular to the longitudinal axis of the trunk (Fig. 1). Taking the sine of the mean θ for all tests (Table 1) indicated that 97 % of the load was applied normal to the long axis of the trunk and induced a bending moment.

We attached a strain meter to the side of the trunk opposite of the applied load approximately 1 m above ground as described by James and Kane (2008). The instrument recorded axial displacements, which we converted to strains (ε), at 20 Hz. To relate displacements to loads, we averaged two successive displacements for the load at each 0.1 s. We conducted two pull tests on each tree. To ensure that induced stresses remained in the elastic range, in the first test, we winched trees to induce axial displacements at the height of the strain meter of approximately 1–2 mm. The load–displacement curves (Fig. 2) confirmed this; there was no evidence of plastic deformation after we released tension in the rope. In the second test, we removed the strain meter and winched trees until they failed. For both tests, the rate of loading varied with trees of different dimensions and the time in the test. Loading rate ranged from approximately 100–200 N/s, which induced displacements at a rate of approximately 0.1–0.2 mm/s.

Sixteen trunks split into co-dominant stems higher in the crown and we applied the load to one of the pair. We randomly chose to apply the load parallel ($n = 8$) or perpendicular ($n = 8$) to the plane that bifurcated the co-dominant union. Of the latter, we randomly chose to apply the load to pull the co-dominant stems apart ($n = 5$) or together ($n = 3$). We calculated the relative width of included bark as the ratio of the maximum width of included bark to the width of the cross section.

In the first test, we calculated stress (σ_{BH}) as the sum of the induced axial and bending stresses at breast height (1.4 m above ground):

$$\sigma_{BH} = \frac{P_1 \cos\theta}{\pi r_{BH}^2} + \frac{r_{BH} P_1 l_{BH} \sin\theta}{I_{BH}}, \quad (1)$$

where P_1 is the applied load (twice the value recorded on the load cell), l_{BH} is the distance between the applied load and breast height, θ is the angle between the applied force and the trunk, and r_{BH} and I_{BH} are the radius and area moment of inertia of the trunk at breast height, respectively. We assumed that the trunk cross section was circular. We fitted a least squares regression line to the plot of σ_{BH} and ε during the first test; the slope of the line is the elastic modulus of the tree at breast height (E_{TREE}). We did not measure the elastic modulus of eight trees because the data logger malfunctioned.

To simulate decay in the trunk on a random subsample of 28 trees, after the first test, we used a chainsaw to cut voids in the trunk at the height of the strain meter. We randomly cut voids as rectangular or parabolic prisms of varying dimensions (Fig. 3; Table 1). The length of the void was perpendicular to both the direction of winching and the longitudinal axis of the trunk. We calculated the area moment of inertia of stems with voids before (I_B) and after (I_A) sawing as described in Ciftci et al. (2014). We calculated the loss in area moment of inertia (I_{LOSS}) as:

$$I_{LOSS} = 1 - \frac{I_A}{I_B}. \quad (2)$$

Sawing through the trunk released growth stress, a possible source of error.

Fig. 3 Two examples of voids sawn through trees; trees were pulled to the left

In the second test, excluding trees into which we cut voids, we calculated the maximum value of two types of stress at the point of failure (PF). The first was the sum of axial and bending stress (σ_{PF})

$$\sigma_{PF} = \frac{P_2 \cos\theta}{\pi r_{PF}^2} + \frac{r_{PF} P_2 l_{PF} \sin\theta}{I_{PF}}, \quad (3)$$

where P_2 represented the maximum applied load in the second test (which was twice the value recorded by the load cell), l_{PF} was the distance between the applied load and the point of failure, and r_{PF} and I_{PF} were the radius and area moment of inertia of the trunk at the point of failure, respectively. We assumed that the trunk cross section at the point of failure was circular. The product

$$P_2 l_{PF} \sin\theta \quad (4)$$

is the applied bending moment at the point of failure (M_{PF}). For trees that failed at areas of extant decay, we reduced I_{PF} in Eq. 3 according to the results of Ciftci et al. (2014). Because several trees appeared to fail in shear—indicated by splitting of the member along the neutral axis—rather than bending, we also calculated shear stress at the point of failure (τ_{PF}), assuming a circular cross section:

$$\tau_{PF} = \frac{4 P_2 \sin\theta}{3\pi r_{PF}^2}. \quad (5)$$

For trees that uprooted, we calculated τ_{PF} and σ_{PF} in the trunk above the root flare. This calculation did not represent the actual failure stress for uprooted trees, which would have required a more careful accounting of the root-soil plate, root morphology, and soil texture. Instead, calculating maximum stress in the trunk of uprooted trees (from Eqs. 3, 5) provided a point of comparison with the other types of failure. From the length and width of the overturned root-soil plate, excluding roots that protruded beyond the soil, we calculated its area as an ellipse. From its area and depth, we estimated the volume of the overturned root-soil plate as a right elliptical cylinder.

Laboratory tests

For a random subsample of 34 trees, after completing the second test, we removed a bolt of wood from the trunk at approximately half of its length. We machined four specimens from the outermost growth rings of each bolt: two incident with and two orthogonal to the direction of applied loading. We kept the specimens in sealed plastic bags at 4 °C and measured their moduli of rupture (MOR) and elasticity ($E_{SPECIMEN}$) in a conventional three-point bending test (ASTM 2014). After testing, we removed a cube 3.8 cm on a side from each specimen and measured its mass and volume before and after drying for 3 days at 104 °C. From these measurements, we calculated specific gravity and moisture content as described by Glass and Zelinka (2010).

Analyses

We used stepwise multiple regression analysis to investigate which measures of tree morphometry (DBH, height, crown height, crown width) accounted for a greater proportion of the variability of E_{TREE} (from the first pulling test) and M_{PF} (from the second pulling test). The stepwise procedure iteratively introduced independent variables in order of descending F values, excluding (at each step) variables for which $p(F) > 0.05$. If multiple independent

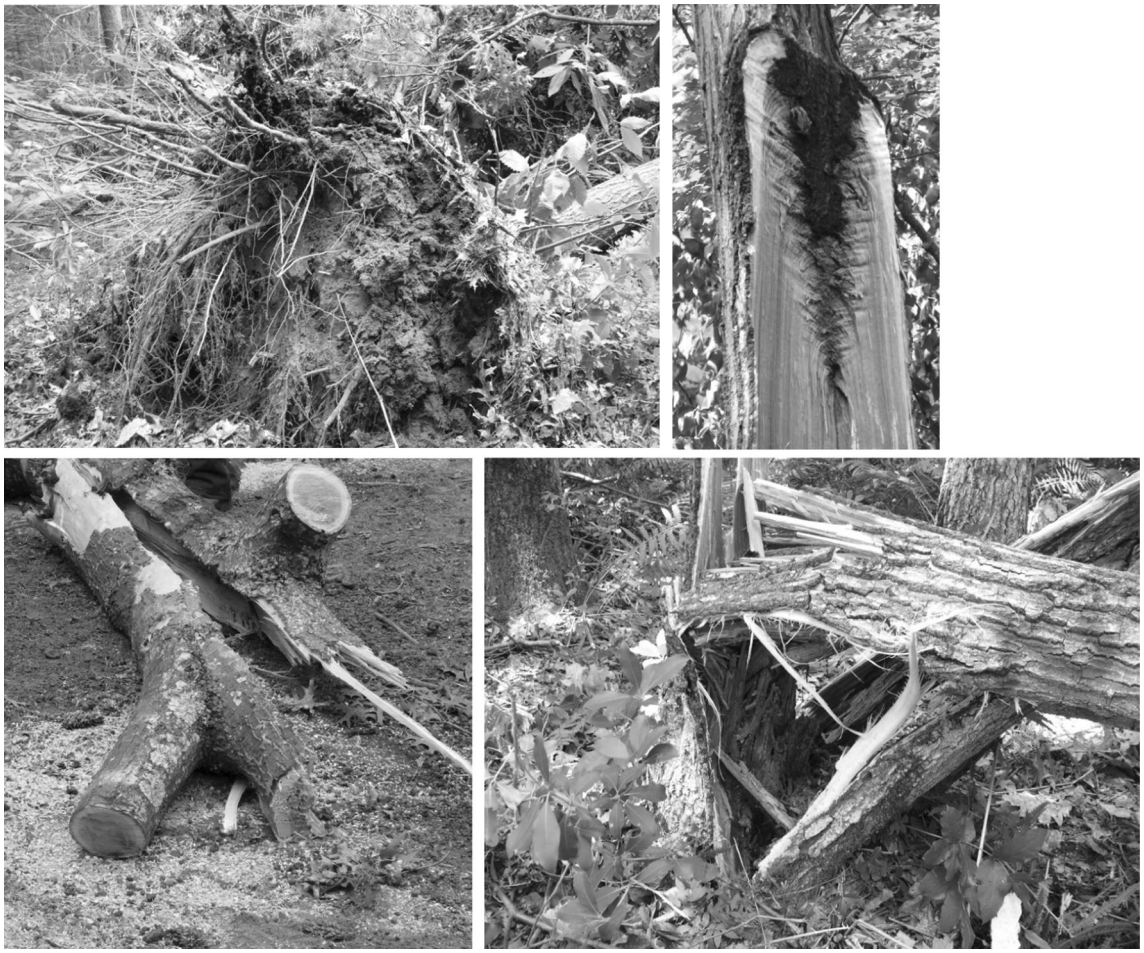

Fig. 4 Four types of failures observed in the study; clockwise from top left: uproot, co-dominant stem, at an area of extant decay, and in the crown in the vicinity of branches

variables were significant in a model, we calculated variance inflation factors to check for multicollinearity. We included all but eight trees in regressions of E_{TREE}. For M_{PF}, we conducted separate regressions for trees that failed in different ways. We observed four types of failures (Fig. 4): uprooting, of the union of co-dominant stems, in the trunk due to extant decay, and in the crown in the vicinity of branches. One tree failed below the crown in the vicinity of a formerly shed branch. We included it with trees that failed in the crown in the vicinity of branches. There were too few trees that failed at areas of extant decay and co-dominant stems to use regression analysis.

For the first pulling test, we used a mixed model analysis of variance (ANOVA) to determine whether the elastic modulus of trees that failed at areas of extant decay (E_{DECAY}) was different from the remaining trees (E_{TREE}). A preliminary analysis showed that E_{TREE} did not differ among failure types of the remaining trees. We included the random effect of tree nested within failure type in the ANOVA.

For the second pulling test excluding trees into which we cut voids, we used a mixed model ANOVA to determine whether the following variables differed among four failure types: distance between the applied load and the point of failure, M_{PF}, I_{PF}, τ_{PF}, and σ_{PF}. We included the random effect of tree nested within failure type in the ANOVA and used the Bonferroni adjustment to separate least squares means when the effect of failure type was significant ($p < 0.05$). Visual examination of plots of residuals revealed that they were not normally distributed in the ANOVAs of M_{PF} and σ_{PF}, which we confirmed using the Shapiro–Wilk test. Analyzing natural-log transformed values of M_{PF} and σ_{PF} normalized the distribution of the residuals. We present non-transformed values in the results. We also used a mixed model ANOVA to determine whether the relative width of included bark differed among co-dominant stems pulled in different directions. We used Fisher's exact test to investigate whether failure of co-dominant stems was associated with the direction of loading. For trees into which we cut voids, we used logistic

Table 2 Least squares means and standard errors (in parentheses) of parameters at the point of failure (PF) for each type of failure

Failure type	n	M_{PF}[a]	σ_{PF}[b]	τ_{PF}[c]	Diameter$_{PF}$	Lever[d]	I_{PF}[e]
Co-dominant stems	4	71.1 (27.1)ac	35.2 (5.68)a	0.23 (0.06)ac	27.8 (3.37)ac	6.95 (1.24)a	3.25 (3.71)ab
Decayed stem	5	23.1 (24.2)b	33.4 (5.08)a	0.49 (0.05)b	26.6 (3.02)ab	6.02 (1.11)a	1.18 (3.32)a
Crown	7	39.5 (22.1)ab	39.1 (4.64)a	0.42 (0.05)ab	21.7 (2.74)ab	3.35 (0.98)a	1.40 (3.03)a
Uproot	21	127 (12.1)c	26.6 (2.48)a	0.14 (0.03)c	36.1 (1.47)c	11.8 (0.54)b	10.6 (1.62)b

Read down each column, least squares means followed by the same letter are not different ($p > 0.05$) using the Bonferroni adjustment for multiple comparisons

[a] Applied bending moment (kNm)

[b] Bending and axial compressive stress (MPa)

[c] Shear stress (MPa)

[d] Distance between the applied load and the point of failure (m)

[e] Area moment of inertia (dm^4)

Table 3 Means and standard deviations (SD) of (a) the elastic modulus of trees with (E_{DECAY}) and without decay (E_{TREE}), (b) wood properties of specimens taken from a random sample of trees, and (c) dimensions of the root-soil plates of uprooted trees

Parameter	Units	n	Mean[a]	SD
(a)				
E_{TREE}	MPa	42	4,590	1,310
E_{DECAY}	MPa	5	3,160	1,540
(b)				
Specific gravity	–	34	0.54	0.03
$E_{SPECIMEN}$[b]	MPa	34	14,600	1,910
MOR[c]	MPa	34	62.6	7.29
(c)				
Area	m^2	20	4.03	2.59
Depth	m	20	0.72	0.30
Volume[d]	m^3	20	3.23	3.03

[a] Values of E_{TREE} and E_{DECAY} are least squares means

[b] Elastic modulus of specimens measured in 3-point bending

[c] Modulus of rupture of specimens

[d] Estimated as a right elliptical cylinder

regression to determine whether the probability of failure occurring at the void was related to the loss in area or I_{LOSS} at the void.

Results

M_{PF} was greater for trees that uprooted than those that failed in the crown or at an area of extant decay (Table 2). It was also greater for failures of co-dominant stems than trees that failed at an area of extant decay (Table 2). These findings were consistent with (1) greater distance between the applied load and point of failure on trees that uprooted and (2) greater diameter at the point of failure of uprooted trees, which increased I_{PF} compared to crown failures and trees that failed at areas of extant decay (Table 2). For the sake of comparison to other types of failure, the point of failure of uprooted trees was considered to be the trunk above the root flare. Equation 3 accounts for differences in I_{PF}, so σ_{PF} did not differ among failure types, but there was a large difference between crown failures and uprooted trees (Table 2). The difference was not significant ($p = 0.095$), presumably due to the small number and greater variability of σ_{PF} of crown failures. Excluding trees that uprooted, σ_{PF} was 57 % of MOR (Table 3). For uprooted trees, σ_{PF} was 40 % of MOR. The best predictor of M_{PF} of uprooted trees was crown width; for crown failures, it was I_{PF} (Table 4).

τ_{PF} was greater for trees with areas of extant decay than failures of co-dominant stems or uprooted trees (Table 2). It was also three times greater for crown failures than uprooted trees (Table 2). τ_{PF} of crown failures was nearly twice as large as failures of co-dominant stems, but the small sample sizes and large variability around both means obscured a statistical difference ($p = 0.125$) (Table 2).

E_{TREE} increased linearly with crown width, but the correlation coefficient was only 0.29 (Table 4). No other morphometric measures were significantly correlated with E_{TREE}. The mean value of $E_{SPECIMEN}$ was more than three times greater than E_{TREE} (Table 3). There was some evidence ($p = 0.053$) that E_{TREE} was greater than E_{DECAY} (Table 3).

Of 34 trees with areas of extant decay ($n = 6$) or sawn voids ($n = 27$), 10 did not fail at the void ($n = 8$) or area of extant decay ($n = 2$). We excluded from the logistic regression one tree with a sawn void that failed at an area of extant decay in the crown. The probability of failure of trees with extant decay or a sawn void increased with I_{LOSS} (Fig. 5). The coefficients of the logit equation quantifying the probability of failure were similar regardless of whether we analyzed only trees with sawn voids or the pooled set of trees with areas of extant decay and sawn voids (data not presented). No trees with less than 22 % I_{LOSS} failed at the

Table 4 Regression statistics for responses and predictors including, the sample size (n) and correlation coefficient (r^2) [adjusted for multiple regression (Adj-R^2)] of each model, as well as the model coefficients [slope (β), intercept (B)] and their standard errors (SE), t, χ^2, and p values

Response	Predictor	Units	n	Adj-R^2	B	SE	t	p	β	SE	t	p
(a)												
E_{TREE}	Crown width	MPa	42	0.29	853	935	0.91	0.367	347	85.2	4.10	0.000
M_{PF}^{a}	Crown width	kN m	20	0.80	−133	30.8	−4.32	0.000	26.5	3.05	8.69	0.000
M_{PF}^{b}	I_{PF}^{c}	kN m	7	0.93	14.0	4.77	2.94	0.032	183	20.7	8.85	0.000

Response	Predictor	n	r^2	B	SE	Wald χ^2	p	β	SE	Wald χ^2	p
(b)											
Failure at void	I_{LOSS}^{d}	42	0.44	−2.32	1.16	3.96	0.047	9.31	3.67	6.43	0.011

[a] Maximum bending moment at the point of failure or trees that failed in the trunk

[b] Maximum bending moment at the point of failure for trees that uprooted

[c] Area moment of inertia measured at the point of failure

[d] Loss in area moment of inertia due to a sawn void

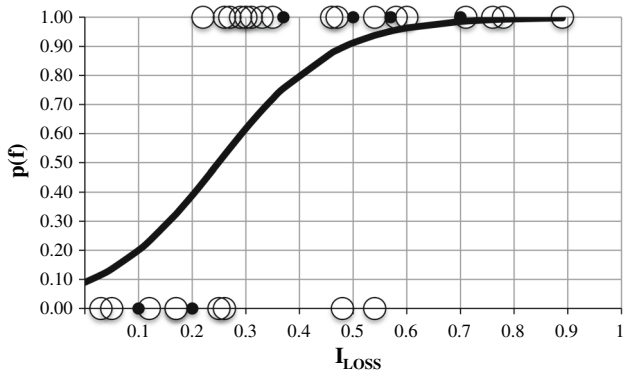

Fig. 5 Trees with sawn voids ($n = 27$, open circles) or extant decay ($n = 6$, filled circles) that did [$p(f) = 1$] or did not [$p(f) = 0$] fail at the sawn void or area of extant decay plotted against the loss in area moment of inertia (I_{LOSS}) due to the void or decay (Eq. 2 in the text). The line indicates the predicted probability of failure [$p(f)$], which was correlated with I_{LOSS}. Table 4 includes coefficients describing the line

area of extant decay or sawn void, and all trees with greater than 54 % I_{LOSS} failed at the area of extant decay or sawn void (Fig. 5). Only 2 trees with I_{LOSS} greater than 30 % did not fail at the sawn void, but four trees failed at the sawn void when the I_{LOSS} was between 22 % and 30 % (Fig. 5). The probability of failure of trees with extant decay or a sawn void was not related to the loss in cross-sectional area (data not presented).

Of five co-dominant stems to which we applied the load perpendicular to the plane bifurcating the co-dominant union and pulling the stems apart, four failed at the union and one uprooted. All of the unions that failed had included bark centered along the width of the plane bifurcating the union (Fig. 4). The co-dominant union that did not fail did not have included bark. None of the three co-dominant stems to which we applied the load perpendicular to the plane bifurcating the co-dominant union and pulling the stems together failed; they all had included bark. None of the eight co-dominant stems to which we applied the load parallel to the plane bifurcating the co-dominant union failed. Six of the eight unions had included bark. The relative maximum width of included bark did not differ among co-dominant stems pulled in three different directions (Table 5). When we applied loads perpendicular to the plane that bifurcated the co-dominant union, failure was more likely to occur than when we applied the load parallel to the plane (Table 5).

Discussion

Assessing the likelihood of tree failure is an important part of arboricultural practice, but very few studies have quantified mechanical parameters like elastic modulus and maximum stress that are necessary to develop mechanistic models of large, open-grown trees, nor have many studies considered large, open-grown trees when quantifying common defects like weak branch unions (Lilly and Sydnor 1995; Kane and Clouston 2008) and decay. Scaling results from small to large trees is problematic because of non-linear relationships between some relevant mechanical parameters and tree size, as well as ontogenetic changes in material properties (Niklas 1997). Our study presents novel data for a species commonly planted in many residential neighborhoods in the USA and eastern Canada.

We expected that the probability of failure at a sawn void would increase as I_{LOSS} increased since bending stress is inversely proportional to the area moment of inertia. This is also why we expected I_{PF} to be strongly correlated with M_{PF} of crown failures. Since most sawn voids were not centered on the cross section, we also expected that the probability of failure at a void would not be related to the loss in area. Practitioners assessing decay must consider the

Table 5 Frequency of failure of co-dominant stems pulled in different directions relative to the plane that bifurcated the union; and least squares means and standard errors (in parentheses) of the relative width of included bark (width of included bark divided by width of the union) in co-dominant unions

Pull direction	n	Width[a]	Failure		Frequency comparison	Pearson χ^2	Fisher's exact p
			Yes	No			
Parallel	8	0.48 (0.10)a	0	8	Parallel–perpendicular apart	9.24	0.007
Perpendicular apart	5	0.49 (0.13)a	4	1	Perpendicular apart–perpendicular together	4.80	0.143
Perpendicular together	3	0.49 (0.17)a	0	3			

[a] Read down the column, least squares means followed by the same letter are not different ($p > 0.99$) using the Bonferroni adjustment for multiple comparisons

area and the location of decay in the cross section (Ciftci et al. 2014), and not assume that areas of decay are concentric (Kane and Ryan 2004). Our observations that no trees with less than 22 % loss in area moment of inertia failed at the void and all trees with greater than 54 % loss in area moment of inertia failed at the void are consistent with mensurative studies of standing and failed trees after storms (Smiley and Fraedrich 1992; Kane 2008) and pulling tests of conifers with small amounts of decay (Achim et al. 2005; Bergeron et al. 2009). Mattheck et al. (1993) similarly observed more failures of trees when two-thirds, as opposed to one-third, of the cross section was sawn. Our findings are also consistent with Coder (1989) who suggested that when the loss in area moment of inertia was between 20 and 45 %, trees should be treated with "caution", and when the loss in area moment of inertia was 45 % or greater, trees should be considered a "hazard". Wagener (1963) suggested that forest-grown conifers were more likely to fail when "strength loss" exceeded approximately 30 %. He calculated strength loss as the ratio of the cube of the diameter of an area of decay to the cube of trunk diameter at the area of decay. The equivalent value expressed as the ratio of area moment of inertia of the cross section with and without decay is 20 %, which is consistent with our findings.

Between 22 and 54 % I_{LOSS}, the likelihood of failure was less predictable, and the non-zero intercept in the logit model indicates that one should interpret our results cautiously. This may have been due to experimental error, although we believe that the effect of releasing growth stress by cutting voids was negligible ("Appendix A"). Cutting voids may have concentrated stress near their apices (Mattheck et al. 1993), but we did not quantify this effect. If they occurred, stress concentrations would have induced failure at a smaller measured I_{LOSS}, which may explain why some trees with small values of I_{LOSS} failed at the void. Since the logit model was similar whether or not we included trees with areas of extant decay in the sample of tree with cut voids, we are less concerned that experimental error confounded our results. Of the two trees with greater than 40 % I_{LOSS} that did not fail at the void, one uprooted and the other failed in the crown. For the latter, σ_{PF} was 12 MPa greater than stress at the sawn void. For the former, σ_{PF} was 10 MPa less than that at the void, but also 3 MPa less than the mean σ_{PF} of uprooted trees. Since there was a large difference in σ_{PF} and τ_{PF} between uprooted trees and crown failures, uprooting was understandable.

The frequency of above-ground failures of red oak was greater than previously reported for other species, mostly conifers (Nicoll et al. 2006; Ruel et al. 2010). Although the mean height of failures of red oak (6.6 m) was substantially greater than previously reported (Fredericksen et al. 1993; Moore 2000; Peltola et al. 2000; Achim et al. 2005), it was similar to large, open-grown maples, none of which uprooted (Kane and Clouston 2008). This finding indicates that branches (including co-dominant stems) play an important role in inducing failure of open-grown trees and is consistent with previous reports (Greig and Gibbs 1990). The correlation between M_{PF} of uprooted trees and crown width has not been previously reported, but crown width of red oaks was correlated with area of the root-soil plate and DBH (data not presented). Both of the latter parameters have been correlated with the maximum bending moment to uproot trees (Papesch et al. 1997; Moore 2000; Peltola et al. 2000; Peterson and Claassen 2013).

Elastic modulus of trees is an important parameter that affects many aspects of mechanical behavior, yet there are very few published values for large, open-grown trees. Instead, published values from specimens [e.g., Kretschmann (2010)] have been used in studies (Ciftci et al. 2013) and in practice (Brudi and van Wassanaer 2001). The smaller value of E_{TREE} for trees that had extant areas of decay, which was consistent with smaller critical bending moments of black spruce [*Picea mariana* (Mill) BSP] with decay (Bergeron et al. 2009), supports the use of pulling tests to assess the effect of decay on the likelihood of failure. However, the large disparity between E_{TREE} and $E_{SPECIMEN}$ suggests that using values from specimens can lead to large errors. Four possible sources of experimental error may have affected our measurement of E_{TREE}. Two of them (non-linear stem deflection near the applied load and

rotation of the root-soil plate) would have overestimated E_{TREE}, but the others (not measuring the bending moment due to offset mass of the deflected stem and measuring diameter outside of the bark) would have underestimated E_{TREE}. During the first pulling test, we did not observe large stem deflections or rotation of the root-soil plate and do not believe that these sources of error confounded our results. In a pulling test, practitioners may not always account for bark thickness, so our results are consistent with field techniques.

The finding that σ_{PF} of co-dominant stems was neither statistically nor practically different from that of crown failures contradicted previous work (Kane and Clouston 2008). Three crown failures occurred in the vicinity of large lateral branches and appeared to fail in shear rather than bending (Fig. 4). Even though shear stress did not statistically differ between crown failures and failures of co-dominant stems, the magnitude of the difference was closer to what Kane and Clouston (2008) observed. The disparity between MOR and σ_{PF} was less than the disparity between $E_{SPECIMEN}$ and E_{TREE}. It was greater than the disparity between MOR and σ_{PF} of maples (Kane and Clouston 2008), but not outside of the range of previously reported disparities [e.g., compare four species in Ruel et al. (2010)]. Although we did not measure maximum shear stress parallel to the grain of specimens, the value for red oak in Kretschmann (2010) was approximately 100 times greater than we measured on crown failures. This provides additional evidence that branches on decurrent trees can serve as defects, and is consistent with the apparent effect of even small branches (recorded as knots) reducing stem resistance to breakage (Ruel et al. 2010).

The union of co-dominant stems appeared to be weaker only when pulled apart, loaded perpendicular to the plane that bifurcated the union, even though the width of included bark was similar for each direction of applied load. Included bark tends to weaken branch unions (Smiley 2003), but the amount has not been conclusively correlated with the reduction in strength (Kane et al. 2008). We expected the effect of included bark to be greater when we loaded co-dominant stems perpendicular to the plane bifurcating the union because the maximum width of included bark coincided with the neutral axis of the trunk (Fig. 6), where shear stress is greatest. When loading parallel to the plane bifurcating the co-dominant union, the maximum width of included bark was perpendicular to the neutral axis of the trunk (Fig. 6), so its effect would be minimal. Pulling co-dominant stems apart also induces tensile stress perpendicular to the plane bifurcating the co-dominant union. When included bark occurred in co-dominant unions, it was centered along the width of the union (Figs. 4, 6). In the center of the union, the absence of

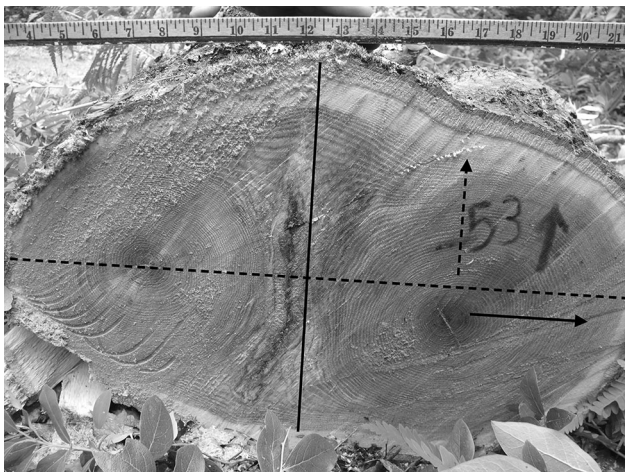

Fig. 6 Cross section of the union of co-dominant stems with included bark. *Black arrows* indicate the direction of loading: the *solid arrow* coincides with a load applied perpendicular to the plane bifurcating the union, pulling the stems apart; the *dashed arrow* coincides with a load applied parallel to the plane bifurcating the union. The *solid and dashed lines* indicate the approximate location of the neutral axis of the cross-section with a load applied perpendicular and parallel to the plane bifurcating the union, respectively

fibers can significantly reduce the strength of the union (Slater and Ennos 2013). This effect did not exist when pulling co-dominant stems together because the stress perpendicular to the plane bifurcating the union was compressive. Since shear stress would be similar whether stems were pulled together or apart, tensile stress perpendicular to the plane bifurcating the co-dominant union appeared to govern the likelihood of failure.

Patterns of failure of red oaks differed from previous reports on mostly coniferous trees growing in forests or plantations; fewer trees uprooted and more failed in the crown, illustrating the importance of considering crown failures on open-grown trees of decurrent form. Our work clarified the effect of two common defects of trees growing in residential settings, decay and co-dominant stems, which will be useful to practitioners who must assess the likelihood of failure. Much work remains to be done, however, since the range of values of I_{LOSS} for which it was harder to predict the likelihood of red oaks failing at a void corresponds to a wide range of areas of decay (Ciftci et al. 2014). Destructively testing trees with extant decay is an important line of future investigation. Long-term tree pulling studies that cover a range of species and sites (Nicoll et al. 2006; Ruel et al. 2010), have provided copious data on which mechanistic models to predict tree failure in forest stands have been built (Peltola 2006). Analogous empirical data for open-grown trees commonly grown in residential neighborhoods would be of great help in developing models to predict failure of such trees.

Author contribution statement B. Kane conducted the experiment, analyzed the results, and wrote the manuscript.

Acknowledgments The TREE Fund's Dr. Mark S. McClure Fellowship in Tree Biomechanics partially funded this study. The author gratefully acknowledges the following individuals who helped collect data: Dan Pepin, Alex Julius, Alex Sherman, Joseph Scharf, Nevin Gomez, and Sherry Hu (University of Massachusetts-Amherst), and Dr. Cihan Ciftci (Abdullah Gul Uinversity, Turkey) for calculating area moments of inertia. The author also thanks Professor Jean-Claude Ruel (Université Laval), two anonymous reviewers, and the Communicating Editor for critically reviewing previous drafts.

Conflict of interest None declared.

Appendix A

In standing trees, the effect of axial growth stress is additive to axial and wind-induced bending stresses. Axial stress due to self-weight is uniformly compressive throughout the cross section. Bending stresses are tensile and compressive, and their magnitude is greatest at the circumference of the cross section. Growth stresses are compressive near the pith and maximally tensile at the circumference of the cross section. During the winching tests, tensile growth stress at the circumference of the cross section counteracts the combined compressive axial and bending stress due to self-weight and the test itself. We used two methods to estimate the combined effect of axial compressive stress due to self-weight and tensile growth stress and compared it to the total compressive stress (axial and bending) induced by winching.

In the first method, we gleaned values of axial tensile growth stress from the literature. On stems of oaks growing without a lean, the magnitude of axial tensile growth stress was about 6 MPa (Wilhelmy and Kubler 1973; Yao 1979), similar to the value reported for the compression side of a leaning red oak (Okuyama et al. 1994). Since none of the measured red oaks expressed a lean, we assumed the value of 6 MPa. Next, we estimated axial compressive stress due to self-weight from (1) the volume of the stem above the height at which we sawed the void, (2) the density of the wood measured from green specimens sampled from the tree, and (3) the cross-sectional area of the stem excluding the sawn void. For each tree, we subtracted axial compressive stress due to self-weight from tensile growth stress of 6 MPa.

In the second method, we calculated the difference between baseline axial displacements (i.e., before applying the load, but after branches were pruned) before and after we cut voids into the trees. For each tree, we converted the difference to a strain and multiplied by the elastic modulus of green specimens sampled from the tree and tested in 3-point bending (ASTM 2014). This estimated the combined effect of axial compressive stress due to self-weight and axial tensile growth stress after notching. For either method and all trees, the maximum ratio of (1) the combined effect of axial compressive stress due to self-weight and tensile growth stress to (2) the total compressive stress (axial and bending) induced while winching the tree to failure was 0.002.

References

Achim A, Ruel J, Gardiner B, Laflamme G, Meunier S (2005) Modelling the vulnerability of balsam fir forests to wind damage. For Ecol Manage 204:37–52

ASTM (2014) Standard test methods for small clear specimens of timber D-143-09 (2014). ASTM International, West Conshohocken

Bergeron C, Ruel J, Élie J, Mitchell S (2009) Root anchorage and stem strength of black spruce (Picea mariana) trees in regular and irregular stands. Forestry 82:29–41

Brudi E, van Wassanaer P (2001) Trees and statics: nondestructive failure analysis. In: Smiley ET, Coder K (eds) Tree structure and mechanics conference proceedings: how trees stand up and fall down. International Society of Arboriculture Champaign, IL, pp 53–69

Ciftci C, Brena S, Kane B, Arwade S (2013) Effects of crown architecture on dynamic behavior of decurrent trees: understanding the relationship between branches and stem. Trees 27:1175–1189

Ciftci C, Kane B, Brena SF, Arwade SR (2014) Loss in moment capacity of tree stems induced by decay. Trees 28:517–529

Coder KD (1989) Should you or shouldn't you fill tree hollows? Grounds Maint 24:68–70

Fredericksen TS, Williams RL, Hedden SA (1993) Testing loblolly pine wind firmness with simulated wind stress. Can J For Res 23:1760–1765

Gardiner B, Byrne K, Hale S, Kamimura K, Mitchell SJ, Peltola H, Ruel J (2008) A review of mechanistic modelling of wind damage risk to forests. Forestry 81:447–463

Gilman EF (2003) Branch-to-stem diameter ratio affects strength of attachment. J Arboric 29:291

Glass SV, Zelinka SL (2010) Moisture relations and physical properties of wood, In: Wood handbook, wood as an engineering material (Chapter 4) Department of Agriculture, Forest Service, Forest Products Laboratory, Madison

Greig BJW, Gibbs NJ (1990) Survey of parkland trees and the great storm of October 16, 1987. Arboric J 14:321

James KR, Kane B (2008) Precision digital instruments to measure dynamic wind loads on trees during storms. Agric For Meteorol 148:1055–1061

Kane B (2008) Tree failure following a windstorm in Brewster, Massachusetts, USA. Urb For Urb Green 7:15–23

Kane B, Clouston PL (2008) Tree pulling tests of large shade trees in the genus Acer. Arboric Urb For 34:101–109

Kane B, James KR (2011) Dynamic properties of open-grown deciduous trees. Can J For Res 41:321–330

Kane B, Ryan D (2004) The accuracy of formulas used to assess strength loss due to decay in trees. J Arboric 30:347–356

Kane B, Farrell R, Zedaker SM, Loferski JR, Smith DW (2008) Failure mode and prediction of the strength of branch attachments. Arboric Urb For 34:308–316

Kane B, Modarres-Sadeghi Y, James KR, Reiland M (2014) Effects of crown structure on the sway characteristics of large decurrent trees. Trees 28:151–159

Kretschmann DE (2010) Mechanical properties of wood, In: Wood handbook, wood as an engineering material (Chapter 5) Department of Agriculture, Forest Service, Forest Products Laboratory, Madison, WI

Lilly S, Sydnor TD (1995) Comparison of branch failure during static loading of silver and Norway maples. J Arboric 21:302–305

Mattheck C, Bethge K, Schafer J (1993) Safety factors in trees. J Theor Biol 165:185–189

Moore JR (2000) Differences in maximum resistive bending moments of Pinus radiata trees grown on a range of soil types. For Ecol Manage 135:63–71

Mortimer MJ, Kane B (2004) Hazard tree liability in the United States: uncertain risks for owners and professionals. Urb For Urb Green 2:159–165

Nicoll BC, Gardiner BA, Rayner B, Peace AJ (2006) Anchorage of coniferous trees in relation to species, soil type, and rooting depth. Can J For Res 36:1871–1883

Niklas KJ (1997) Size- and age-dependent variation in the properties of sap- and heartwood in black locust (*Robinia pseudoacacia* L.). Ann Bot 79:473–478

Nowak DJ, Dwyer JF (2000) Understanding the benefits and costs of urban forest ecosystems. In: Kuser JE (ed) Handbook of urban and community forestry in the northeast. Plenum Publishers, NY, pp 11–25

Nowak DJ, Stevens JC, Sisinni SM, Luley CJ (2002) Effects of urban tree management and species selection on atmospheric carbon dioxide. J Arboric 28:113–122

Okuyama T, Yamamoto H, Yoshida M, Hattori Y, Archer R (1994) Growth stresses in tension wood: role of microfibrils and lignification. Ann For Sci 51(3):291–300

Papesch AJG, Moore JR, Hawke AE (1997) Stability of *Pinus radiata* trees at Eyrewell Forest investigated using static tests. New Zealand J For Sci 27:188–204

Peltola HM (2006) Mechanical stability of trees under static loads. Am J Bot 93:1501–1511

Peltola H, Kellomaki S, Hassinen A, Granander M (2000) Mechanical stability of Scots pine, Norway spruce and birch: an analysis of tree-pulling experiments in Finland. For Ecol Manage 135:143–153

Peterson CJ, Claassen V (2013) An evaluation of the stability of *Quercus lobata* and *Populus fremontii* on river levees assessed using static winching tests. Forestry 86:201–209

Ruel J-C, Achim A, Herrera R, Cloutier A (2010) Relating mechanical strength at the stem level to values obtained from defect-free wood samples. Trees 24:1127–1135

Schmidlin TW (2009) Human fatalities from wind-related tree failures in the United States, 1995–2007. Nat Hazards 50:13–25

Slater D, Ennos AR (2013) Determining the mechanical properties of hazel forks by testing their component parts. Trees 27:1515–1524

Smiley ET (2003) Does included bark reduce the strength of codominant stems? J Arboric 29:104–106

Smiley ET, Fraedrich BR (1992) Determining strength loss from decay. J Arboric 18:201–204

Wagener WW (1963) Judging hazard from native trees in California recreational areas: a guide for professional foresters. USFS research paper PSW-P1, 29 p. pacific southwest forest and range experiment station, forest service, US Dept. of Agriculture, Berkeley, Calif

Wilhelmy V, Kubler H (1973) Stresses and checks in log ends from relieved growth stresses. Wood Sci 6:136–142

Yao J (1979) Relationships between height and growth stresses within and among white ash, water oak, and *Shagbark hickory*. Wood Sci 11:246–251